

# Microspherical ReS<sub>2</sub> as a High-Performance Hydrodesulfurization Catalyst

J. A. Aliaga<sup>1,2</sup> · T. N. Zepeda<sup>3</sup> · B. N. Pawelec<sup>4</sup> · J. F. Araya<sup>5</sup> · J. Antúñez-García<sup>6</sup> · M. H. Farías<sup>3</sup> · S. Fuentes<sup>3</sup> · D. Galván<sup>3</sup> · G. Alonso-Núñez<sup>3</sup> · G. González<sup>7,8</sup>

Received: 2 February 2017 / Accepted: 1 March 2017  
© Springer Science+Business Media New York 2017

**Abstract** An unsupported microspherical ReS<sub>2</sub> catalyst, consisting in self-assembled nano-layers, was evaluated in the hydrodesulfurization (HDS) of 3-methylthiophene showing an excellent catalytic activity. The samples were characterized by X-ray diffraction, scanning electron microscopy, high resolution electron microscopy, energy dispersive X-ray spectroscopy and X-ray photoelectron spectroscopy. These techniques revealed that the rhenium disulfide layers are confined to a 3D hierarchical structure with different stacking, slab size and bending, according to

the annealing temperature (400 or 800 °C). The presence of a defect-rich structure in the microspheres, with short and randomly-orientated ReS<sub>2</sub> slabs, results in the exposure of additional edge sites, which improve the catalytic performance of this material. This microspherical ReS<sub>2</sub> composite, with good HDS performance, is a promising catalyst for the desulfurization of fuel oils; the solvothermal reaction conditions are also useful to tune and create exotic morphologies for the design of new ReS<sub>2</sub> catalysts.

**Electronic supplementary material** The online version of this article (doi:[10.1007/s10562-017-2024-6](https://doi.org/10.1007/s10562-017-2024-6)) contains supplementary material, which is available to authorized users.

✉ J. A. Aliaga  
jaliaga@utem.cl

<sup>1</sup> Programa Institucional de Fomento a la Investigación, Desarrollo e Innovación (PIDi), Universidad Tecnológica Metropolitana, Ignacio Valdivieso 2409, San Joaquín, Santiago, Chile

<sup>2</sup> Departamento de Química, Universidad Tecnológica Metropolitana, Las Palmeras 3360, Ñuñoa, Santiago, Chile

<sup>3</sup> Centro de Nanociencias y Nanotecnología, Universidad Nacional Autónoma de México, Km. 107 Carretera Tijuana-Ensenada, Ensenada, Baja California, Mexico

<sup>4</sup> Instituto de Catálisis y Petroleoquímica, CSIC, c/Marie Curie 2, L10, Cantoblanco, 28049 Madrid, Spain

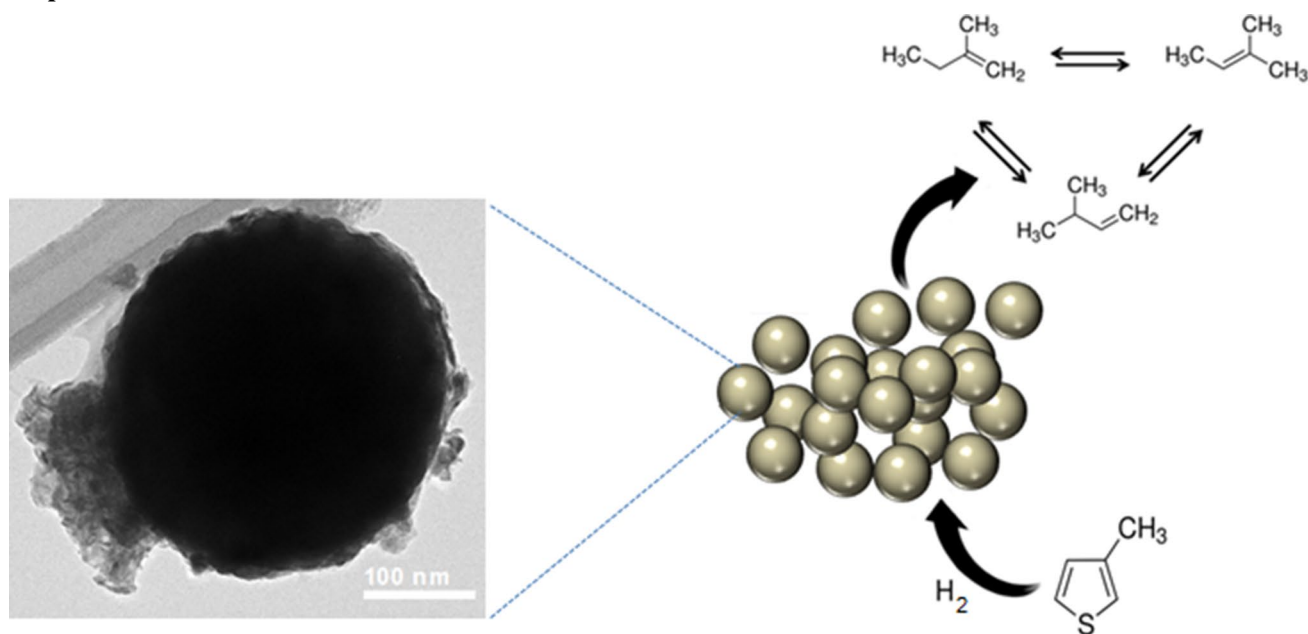
<sup>5</sup> Universidad de Atacama, Copayapu 485, Copiapó, Chile

<sup>6</sup> Centro de Enseñanza Técnica y Superior, Centro de Ingeniería Aplicada, Av. CETYS Universidad, No. 4, Apdo, 1196, Tijuana, Baja California, Mexico

<sup>7</sup> Departamento de Química, Facultad de Ciencias, Universidad de Chile, Las Palmeras 3425, Ñuñoa, Santiago, Chile

<sup>8</sup> Center for the Development of Nanoscience and Nanotechnology, CEDENNA, Santiago, Chile

## Graphical Abstract



**Keywords** Rhenium disulfide · Hidrodesulfurization · Heterogeneous catalysis · Solvothermal synthesis

## 1 Introduction

There is a great interest in the research on the catalytic applications of ReS<sub>2</sub>-based materials for hydrotreating and water splitting reactions, as alternatives to classical MoS<sub>2</sub>-based catalysts [1–3]. This is in part due to the structural similarity between both sulfides, and the unique combination of physical and chemical properties of rhenium and its alloys, making them highly attractive for preparation of novel materials and catalysts [4–6]. Generally, unsupported ReS<sub>2</sub> catalysts show intermediate hydrodesulfurization (HDS) activity in comparison to the sulfides of the group VI and VIII [7, 8]; a similar trend is observed in the Hydrogen Evolution Reaction for this dichalcogenide in comparison to its layered transition metal analogues (MoS<sub>2</sub> and WS<sub>2</sub>) [9]. The differences in the catalytic behavior of the ReS<sub>2</sub> compared with other typical layered transition metal sulfides has been explained by considering the different crystalline structure and electronic properties among these catalysts [9, 10]. ReS<sub>2</sub> has a layered graphite-like structure, where the S–Re–S layers are stacked and held together in the direction perpendicular to their basal plane, joined by van der Waals forces [11]. In particular, the electronic and vibrational behavior of ReS<sub>2</sub> in bulk has been shown to resemble that of the single layer [12].

ReS<sub>2</sub> can be synthesized in several structures; including crystalline layered [13] and inorganic fullerene-like materials [14], colloidal nanoparticles [15, 16], as layered

compounds supported onto carbon nanotubes [17] and as solid microspheres [18, 19], among others. The extremely weak van der Waals coupling and anisotropy of ReS<sub>2</sub> might explain the extreme morphological effect of the disordered lattice structure of this compound in comparison with all the LTMS [10, 20, 21]. Synthetic methods which lead to the formation of disordered, poorly stacked and small-sized layers (including sonochemical and solvothermal syntheses) have shown improvement in the catalytical performance of these materials [22, 23]. These methods also promote the formation of curved or strained layers, which might create new active sites on the basal planes, influencing the HDS activity and selectivity [24, 25].

In this work we tested the catalytic performance of a ReS<sub>2</sub> microspherical material, which was synthesized by a solvothermal process, with the aim to obtain poorly stacked layers with some degree of curvature and a high proportion of edge sites. The as-prepared microspherical ReS<sub>2</sub> catalyst was annealed at 400 and 800 °C, in order to evaluate the effects of temperature over the different layer arrangements and of the crystallinity of the compounds. The catalyst performances of the annealed samples were also compared against a commercial supported Mo/γ-Al<sub>2</sub>O<sub>3</sub> sulfide catalyst.

## 2 Experimental

### 2.1 Catalysts Preparation

In order to obtain ReS<sub>2</sub> microspheres, 0.3 mmol of analytically pure Re<sub>2</sub>(CO)<sub>10</sub>, 6.0 mmol of sulfur powder (excess)

and about 2.5 mL of toluene were put into a Teflon-lined 3 mL stainless steel autoclave and heated in an electrical oven for 24 h at 180 °C. The mixture was then cooled down naturally, giving a black powder. The product was washed twice with both the reaction solvent and diethyl ether, and then was filtered and dried in vacuum for 10 h. The annealing of the sample was carried out by heating it at a rate of 2 °C per min in a conventional tube furnace under Ar flow (20 mL min<sup>-1</sup>) up to 400 °C, and then maintained at this temperature for 1 h. The same annealing procedure was followed for the sample annealed at 800 °C.

## 2.2 Characterization and Activity Measurements

X-ray diffraction (XRD) measurements of the samples were gathered in a Philips spectrometer model X'pert using the Cu K $\alpha$  radiation (40 kV, 30 mA) with wavelength of 0.154 nm. Scanning Electron Microscopy (SEM) micrographs were obtained in a SEM LEO 1420VP, Oxford Instruments, equipped with an energy-dispersive X-ray spectroscopy (EDS) system. HRTEM analyses were performed by means of a JEOL 2010 (200 kV) microscope. X-ray photoelectron spectra (XPS) were carried out in a SPECS custom made system using a PHOIBOS 150 WAL hemispherical analyzer and a  $\mu$ -FOCUS 500 X-Ray source. Charge referencing was done against adventitious carbon (C 1s 284.8 eV). Re 4f and S 2p energy regions were scanned with several sweeps until a good signal-to-noise ratio was observed.

Hydrodesulfurization of 3-methyl-thiophene was carried out in vapor phase using a home-made fixed bed micro flow reactor (15 mm ID) housed in a furnace. The reactor was loaded with 100 mg of catalyst (particle size between 80 and 120 mesh) diluted with 1 g of SiC. Prior to the catalytic test, the catalyst were dried under a N<sub>2</sub> flow of 50 mL min<sup>-1</sup> at 150 °C for 0.5 h to eliminate the moisture, which could be adsorbed on the catalyst surface. The reaction was carried out in atmospheric pressure, and at different temperatures between 280 and 340 °C. Meanwhile, the saturation of hydrogen with 3-methyl-thiophene was obtained by bubbling hydrogen (70 mL min<sup>-1</sup>) through a saturator containing liquid 3-methyl-thiophene at 20 °C (reaching the mole concentration typical to 3-methyl-thiophene saturated to 0 °C). For each catalyst studied, steady state conditions were reached after 1 h of time on-stream reaction. Reaction products were analyzed using an online gas chromatograph (Agilent-7820, FID) equipped with a DB-1 column (30 m length).

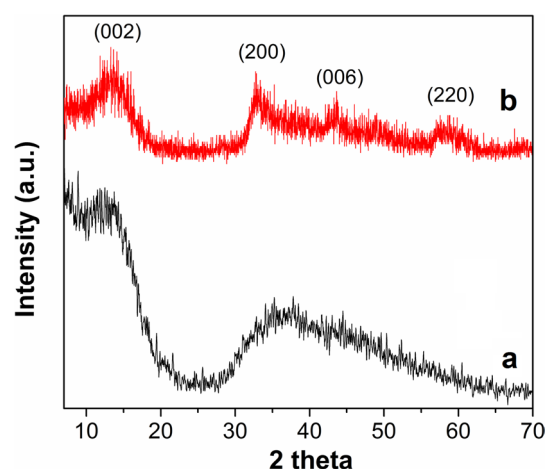


**Fig. 1** XRD patterns of rhenium sulfide microspheres annealed at 400 °C (a) and at 800 °C (b) for 1 h under argon atmosphere

## 3 Results and Discussion

### 3.1 Characterization of Catalysts

#### 3.1.1 X-ray Diffraction Analysis

The influence of the annealing over the as-prepared compound was evaluated using X-ray diffraction. The measured XRD patterns of ReS<sub>2</sub> microspheres treated at 400 and 800 °C are shown in Fig. 1; the annealed sample at 400 °C show broad diffraction peaks, which are mainly located in a low angle region (about  $2\Theta = 13^\circ$ ), and a broad envelope starting at  $2\Theta = 30^\circ$  and lasting out to about  $2\Theta = 60^\circ$ . The ReS<sub>2</sub> (002) plane is broadened, indicating a low stacking of the crystallites along their basal plane, while that the broad peaks between  $2\Theta = 30^\circ$  and  $60^\circ$  are not well resolved, due to the small basal plane sizes and the amorphous nature of the compound [15]. The ReS<sub>2</sub> sample treated at 800 °C (Fig. 1b) shows an improvement in the crystallinity, indicating a growing and stacking of the rhenium disulfide layers; the broad peak between  $2\Theta = 30^\circ$ – $60^\circ$ , observed at 400 °C, resolves into four broad low intensity peaks which correspond closely to the (200), (006) and (220) planes of triclinic ReS<sub>2</sub> [26]. A lattice expansion, characteristic of strained and curved layers, is also observed in the shift of the (002) reflection to a lower angle ( $2\Theta = 13^\circ$ ,  $94^\circ$ ) [27].

#### 3.1.2 HRTEM Analysis

The surface morphology and structure of the ReS<sub>2</sub> sample annealed at 400 and 800 °C were investigated by SEM

**Fig. 2** SEM overview of microspheres annealed at 400 °C (**a**) and TEM details of the border of a microsphere (**b**)

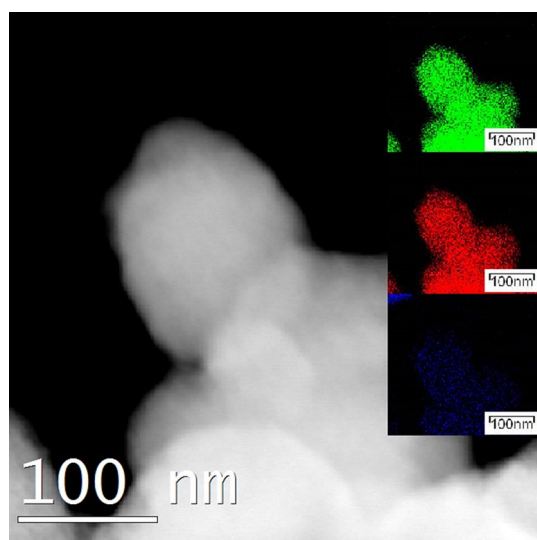
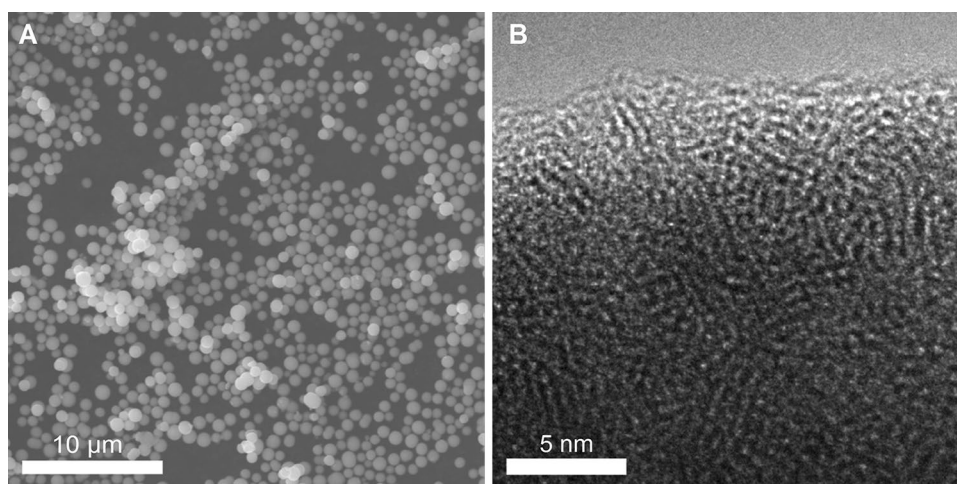


**Fig. 3** Selected image for X-ray dot mapping for ReS<sub>2</sub> microspheres annealed at 400 °C: rhenium (green), sulfur (red) and carbon (blue)

and by High Resolution Transmission Electron Microscopy (HRTEM). Figure 2a show an overview of the ReS<sub>2</sub> sample annealed at 400 °C; this sample consists in discrete and smooth microspheres with a mean diameter of 0.79 µm. The microsphere borders, observed in Fig. 2b, show unclosed shells with many open edges at their surfaces, while the interior of the microsphere is composed by a random arrangement of amorphous rhenium disulfide, in agreement with the broadened XRD pattern. EDS mapping indicates a high percentage of rhenium, sulfur, and a lower percentage of carbon, which is homogeneously distributed around the entire microsphere, scaffolding the inorganic structure (Fig. 3).

The influence of the annealing at 800 °C was also evaluated using HRTEM micrographs. Figure 4a shows that the growth of the ReS<sub>2</sub> layers collapses the microspherical structure, protruding from the borders of the microsphere; the rhenium sulfide fringes present a curved and folded structure, with longitudinal sizes <30 nm (Fig. 4b). The

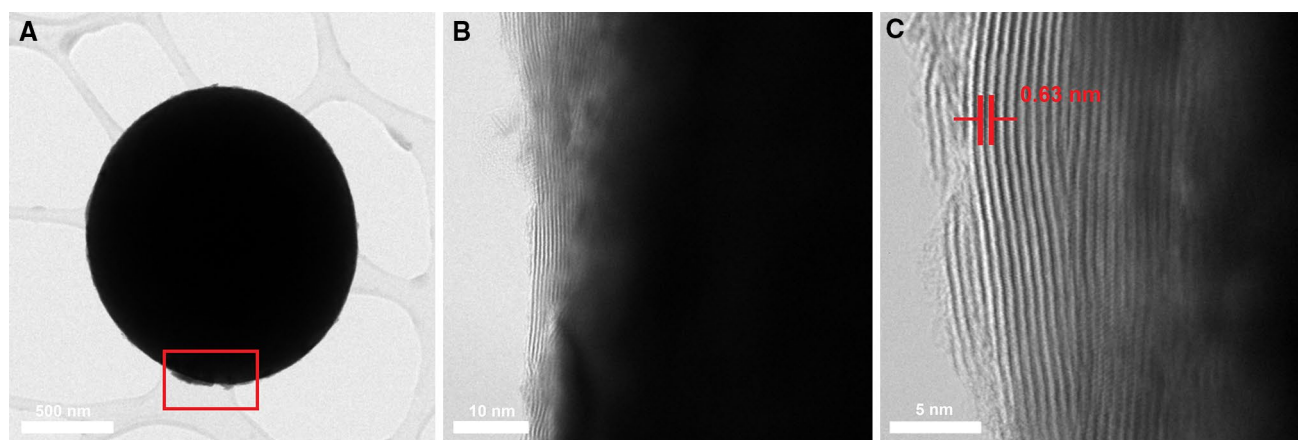
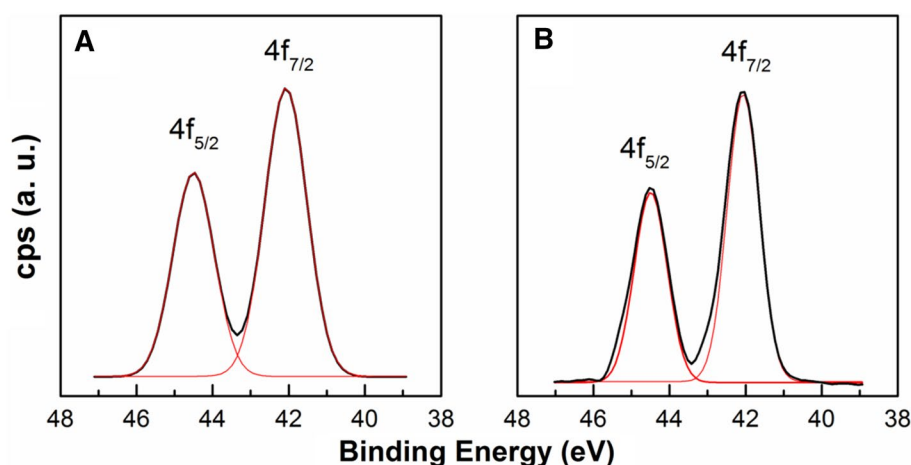


**Fig. 4** TEM of ReS<sub>2</sub> microsphere annealed at 800 °C (**a**) and details of the layers (**b**, **c**). The red square indicates defects on the microspherical structure



**Fig. 5** Re 4f XPS spectra and component fittings of microspherical ReS<sub>2</sub> samples annealed at **a** 400 °C and **b** 800 °C



interlayer distance match the ReS<sub>2</sub> (002) plane (0.64 nm) (Fig. 4c), which corresponds to the interlayer distance expansion found in the XRD diffraction pattern. The EDS analysis (Fig. S1) of the sample treated at 400 °C exhibit a S/Re atomic ratio of 2.46, which indicates an excess of sulfur in the sample; the sample treated at 800 °C shows a lower value for this ratio (2.015) close to the theoretical value which indicates the release of the sulfur excess from the structure.

### 3.1.3 X-ray Photoelectron Spectroscopy

The effect of annealing temperature on the chemical state and surface exposure of ReS<sub>2</sub> catalysts was investigated by X-ray photoelectron spectroscopy, which also corroborated the presence of ReS<sub>2</sub> in the sample. Figure 5a show the XPS spectrum on the region of rhenium for the sample annealed at 400 °C, where the peak at 42.1 eV correspond to the core level Re 4f<sub>7/2</sub>. XPS spectrum of the sample annealed

at 800 °C is shown in Fig. 5b; the presence of Re<sup>+4</sup> can be observed in the core level Re 4f<sub>7/2</sub> peak at 42.3 eV [1]. The binding energy values of the S 2p<sub>3/2</sub> core level of the microspherical ReS<sub>2</sub> annealed at 400 and 800 °C are presented in Table S1. The annealed samples have the S 2p<sub>3/2</sub> peak at 161.8 and 161.9 eV, for the ReS<sub>2</sub>-400 °C and ReS<sub>2</sub>-800 °C samples respectively, which is characteristic of S<sup>2-</sup> ions [1, 18]. The present solvothermal process leads to the formation of pure phases of rhenium disulfide in comparison for example to the sulfidization by H<sub>2</sub>S/H<sub>2</sub> [28].

## 3.2 Activity and Selectivity of Catalysts

### 3.2.1 Hydrodesulfurization Activity

The comparison of the catalysts HDS activities upon steady-state conditions is shown in Fig. 6; all catalysts exhibit an increase of activity as a function of reaction temperature. At a reaction temperature of 340 °C, the

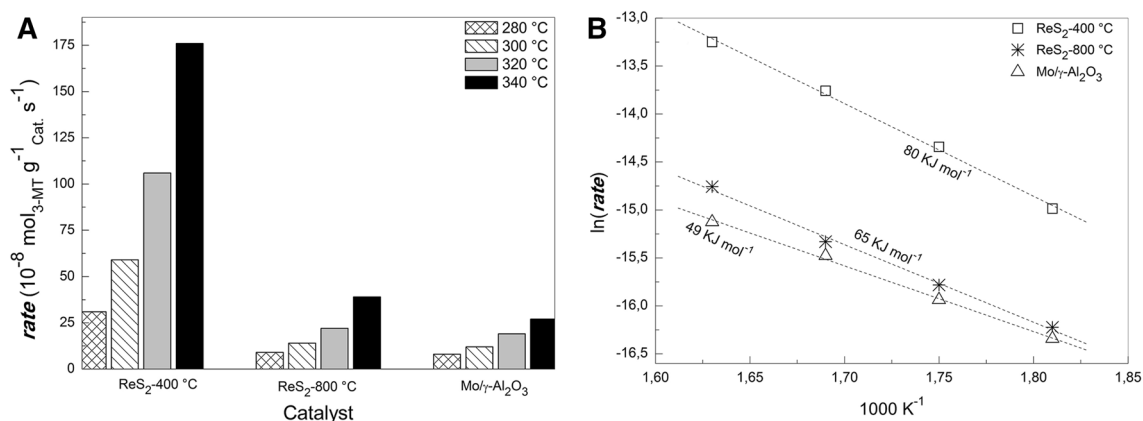


**Fig. 6** HDS of 3-methyl-thiophene over sulfide catalysts (a flow reactor, a steady-state; atmospheric pressure, T=280, 300, 320, 340 °C and conversions between 15–20%) (**a**), Arrhenius plots of the

temperature dependent studies of the HDS of 3-methyl-thiophene over ReS<sub>2</sub> and reference sample (**b**)

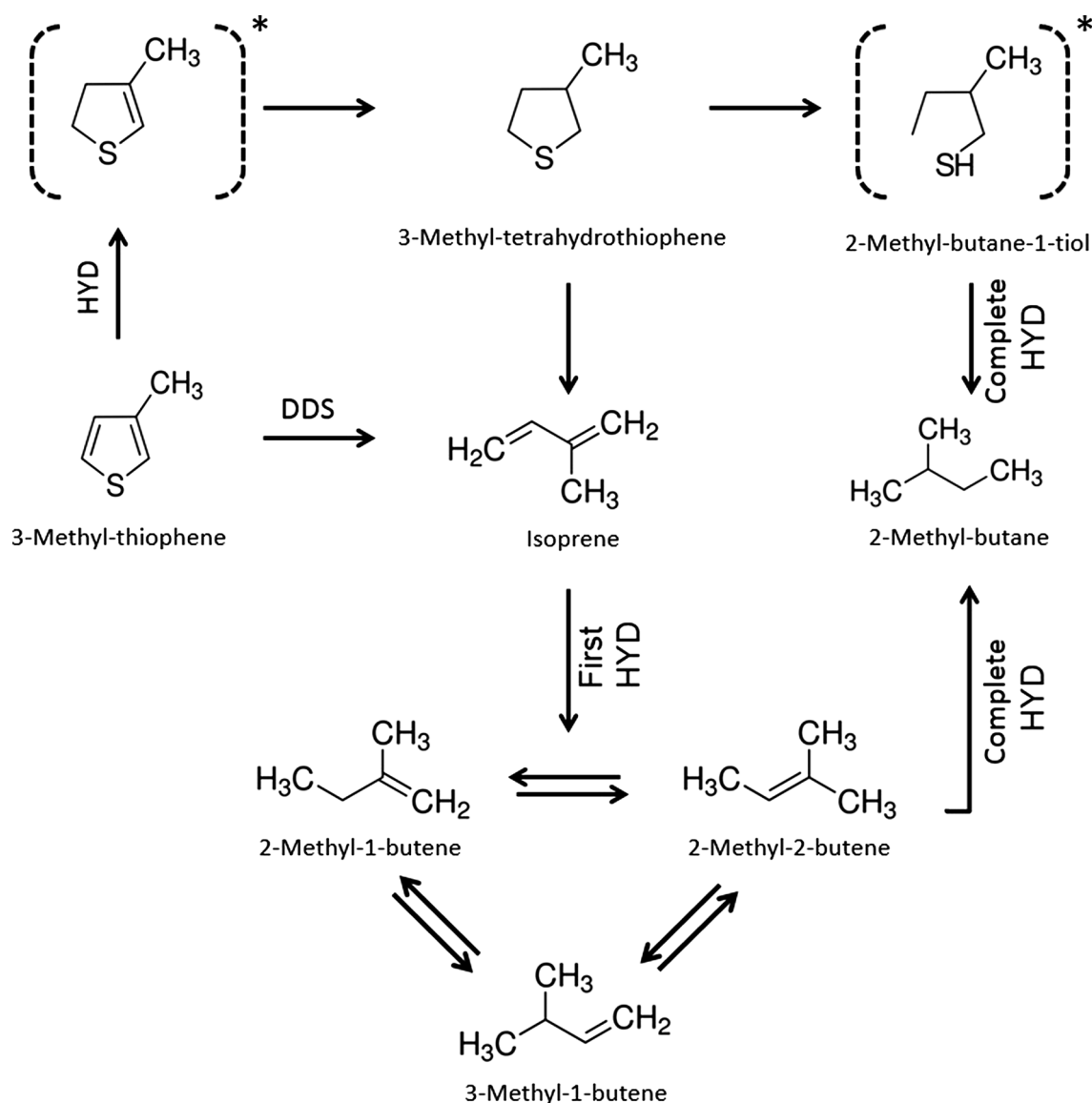


**Fig. 7** Reaction path network for the 3-methyl-thiophene hydrodesulfurization

catalyst activity follows the trend:  $\text{ReS}_2\text{-}400^\circ\text{C} \gg \text{ReS}_2\text{-}800^\circ\text{C} > \text{Mo}/\gamma\text{-Al}_2\text{O}_3$  (Fig. 6a). The Arrhenius plots and the calculations of the apparent activation energy ( $E_{\text{ap}}$ ) for the catalytic reaction are shown in Fig. 6b; the  $E_{\text{ap}}$  follow the trend:  $\text{ReS}_2\text{-}400^\circ\text{C}$  ( $80 \text{ KJ mol}^{-1}$ )  $> \text{ReS}_2\text{-}800^\circ\text{C}$  ( $65 \text{ KJ mol}^{-1}$ )  $\gg \text{Mo}/\gamma\text{-Al}_2\text{O}_3$  ( $49 \text{ KJ mol}^{-1}$ ). Thus, surprisingly, the  $\text{ReS}_2\text{-}400^\circ\text{C}$  exhibit the higher activity and higher apparent activation energy than  $\text{ReS}_2\text{-}800^\circ\text{C}$  counterpart. The same paradoxical behavior reported for  $\text{ReS}_2$  catalysts occurs when the reaction temperatures employed is higher than the isokinetic temperature of the target reaction [29, 30].

### 3.2.2 Selectivity

Under the reaction conditions employed in this work, the reaction products identified were 3-methyl-tetrahydrothiophene (3MTHT), 2-methyl-1,3-butadiene (Isoprene), 3-methyl-1-butene (3M1B), 2-methyl-1-butene (2M1B), 2-methyl-2-butene (2M2B), 2-methyl-butane (2MB), 1-pentene (1P) and mixture (cis- and trans-) 2-pentene (2P). The reaction path network proposed in this work for the HDS of 3-methyl-thiophene (3MT) is shown in Fig. 7, and their possible reactions mechanisms in Fig. S2. Taking into account the products detected, the 3MT transformation over all the studied catalysts proceeds via hydrogenation

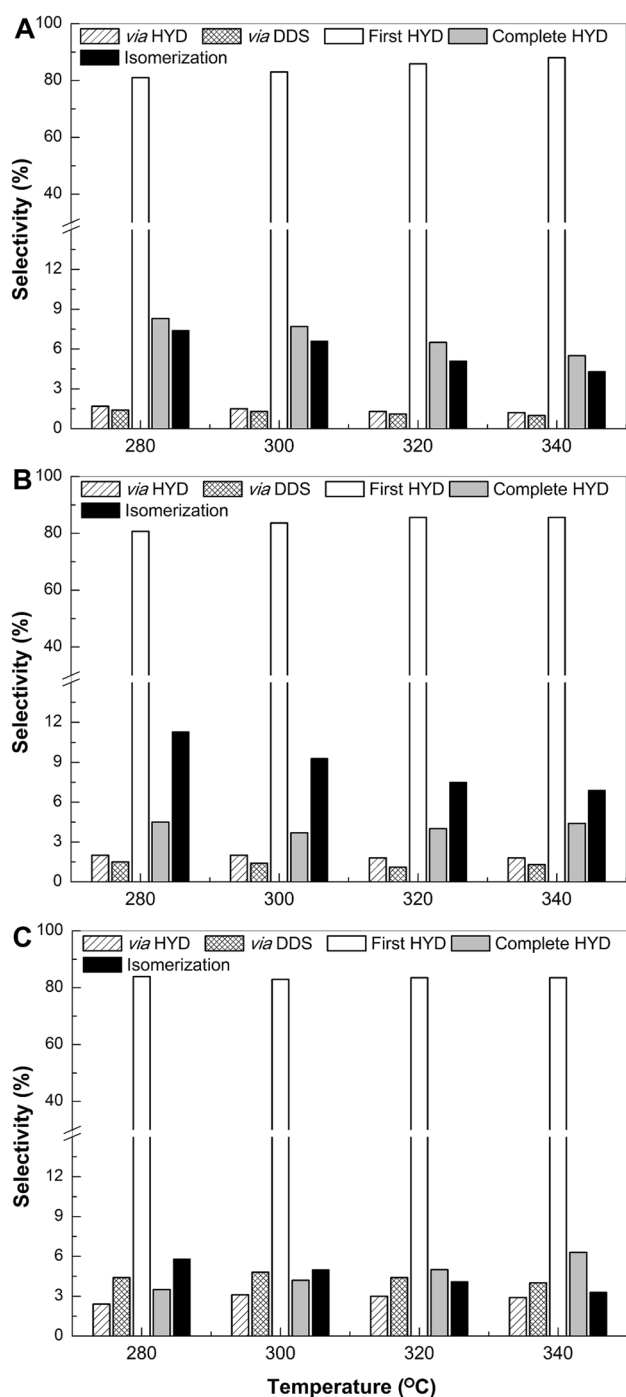


**Fig. 8** Selectivity taken to 20–25% of 3-methyl-thiophene conversion of the  $\text{ReS}_2$  samples annealed at 400 °C (a), 800 °C (b) and  $\text{Mo}/\gamma\text{-Al}_2\text{O}_3$  (c)

(HYD) and direct desulfurization (DDS) reaction pathways. The HYD reaction route led to formation of 3MTHT, isoprene and 2-methyl-butane (2MB). However, isoprene could be formed also via the direct desulfurization reaction route.

Considering the selectivity towards the S-containing product (3MTHT), the catalyst ability for sulfur removal follows the trend:  $\text{ReS}_2\text{-}400^\circ\text{C} > \text{ReS}_2\text{-}800^\circ\text{C} > \text{Mo}/\gamma\text{-Al}_2\text{O}_3$ . The hydrogenation of this compound led to the formation of the mixture of olefins: 3-methyl-1-butene, 2-methyl-2-butene and 2-methyl-1-butene. Their further isomerization led to the formation of 1-pentene and a mixture of cis- and trans-2-pentenenes. For all catalysts studied, the main reaction products were olefins (3M1B, 2M1B and 2M2B). However, the catalysts exhibit a difference in the selectivity towards the formation of complete hydrogenation and isomerization products, including the path of the reaction (DDS and HYD).

The influence of the reaction temperature on the product selectivity (at 3-methyl-thiophene conversion of 20–25%) is shown in Fig. 8. In order to clarify the discussion of the catalytic selectivity results, the DDS and HYD selectivity are defined as selectivity toward isoprene and 3MTHT, respectively, whereas that the olefin mixture (3M1B, 2M1B and 2M2B) were considered as products of the first hydrogenation of their intermediary (isoprene) product. Total hydrogenation was defined considering the selectivity towards 2-methyl butane (2 MB). Finally, to evaluate the contribution of the isomerization reaction pathway, the sum of 1-pentene and mixture of 2-trans(cis)-pentenes was taken into account. By comparing the activity and selectivity of the  $\text{ReS}_2$  samples annealed at 400 °C and 800 °C, it is clear that the annealing treatment influences on both the catalytic activity and the selectivity (Fig. 8a, b). Although the selectivity towards the first hydrogenation products and the hydrodesulfurization via HYD and DDS is comparable in both samples, the sample annealed at 800 °C displayed higher formation of isomerization products and lower complete hydrogenation products than the sample annealed at 400 °C. Although the catalytic activity of the sample annealed at 800 °C is several times lower than its counterpart annealed at 400 °C, its lower hydrogenation ability and higher isomerization properties are attractive characteristics for the production of gasoline. The  $\text{Mo}/\gamma\text{-Al}_2\text{O}_3$  sulfided sample (Fig. 8c) exhibited higher selectivity towards 3MTHT and isoprene than both  $\text{ReS}_2$  samples. Also, the selectivity to the isomerization path was the lowest among the samples, while the selectivity towards the complete hydrogenate products was similar than the  $\text{ReS}_2$  sample annealed at 800 °C. The selectivity results showed improved HDS activity of the  $\text{ReS}_2$  samples, in comparison with the traditional  $\text{Mo}/\gamma\text{-Al}_2\text{O}_3$  sulfided catalyst.

### 3.2.3 Isomerization/Hydrogenation Selectivity's Ratios

In order to obtain more precise information about the isomerization and hydrogenation properties of the catalysts studied, 2 MB/olefin and isomerization/olefin selectivity's

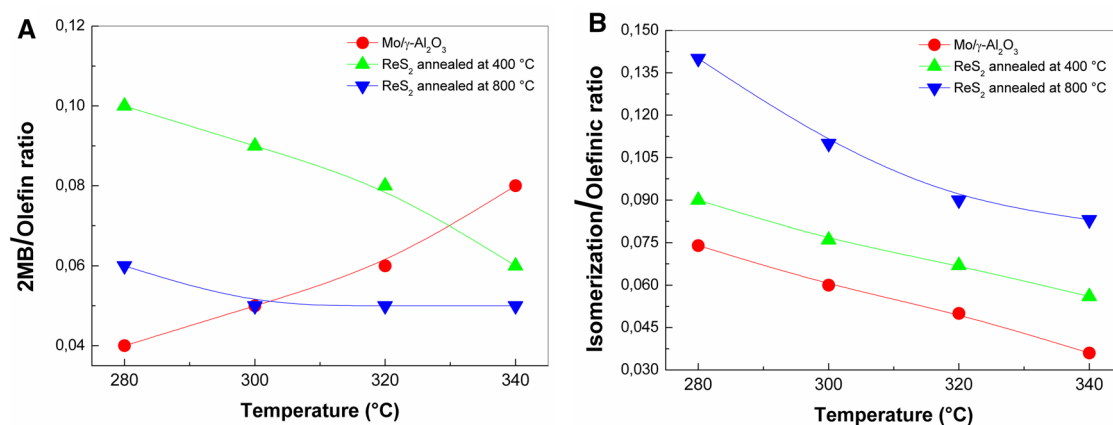


**Fig. 9** **a** 2MB/olefin ratio versus reaction temperature and **b** isomerization/olefin ratio versus reaction temperature

ratios were calculated for the same 3-methylthiophene conversion (20–25%). The total hydrogenation (HYD) was defined considering the selectivity toward 2-methyl butane (2MB) whereas the isomerization reaction pathway was defined as the sum of 1-pentene and mixture of 2-trans(cis)-pentenes.

Figure 9a, b shows the isomerization/olefin and 2MB/olefin selectivity's ratios versus the reaction temperature, respectively. As seen in Fig. 9a, on the contrary to both ReS<sub>2</sub> samples, for the Mo-based catalyst the 2MB/olefin ratio increases with an increase of the reaction temperature. At the highest reaction temperature studied (340 °C), the paraffin/olefin ratio follows the trend: MoS/γ-Al<sub>2</sub>O<sub>3</sub> > ReS<sub>2</sub>-400 °C ≈ ReS<sub>2</sub>-800 °C. This is a very interesting observation because this situation indicates that, by using ReS<sub>2</sub>-based catalysts for the processing of FCC gasoline, the total olefin hydrogenation to paraffin should be avoided. Finally, for all catalysts studied, the isomerization/olefin ratio decreased with an increase of the reaction temperature (Fig. 9b). The ReS<sub>2</sub> sample annealed at 800 °C showed the superior isomerization ability (highest isomerization/olefin ratio), in comparison with the others samples.

Summarizing, taking into account that the catalysts for hydrotreating of FCC gasoline must promote the desulfurization reaction instead of the hydrogenation of olefins, their high HDS activity, low hydrogenation of olefins to paraffins (2-methyl-butane was formed only), and a large isomerization of olefins, the microspherical ReS<sub>2</sub> catalysts are promising catalysts for hydrotreating of FCC gasoline.

### 3.2.4 Factors Influencing on Catalyst Activity

The outstanding HDS activity of the rhenium disulfide annealed at 400 °C can be attributed to the crystalline structure confined into the microsphere, where the amorphous ReS<sub>2</sub> generates an open surface structure with many

reactive edge sites. This sample presents preference for complete hydrogenation reactions, which commonly are associated to edge sites [24]. On the other hand, the sample annealed at 800 °C leads to a significant decrease in activity due to the formation of stacked and longer slabs, which implies a lower proportion of edge sites. With the increase of annealing temperature the ReS<sub>2</sub> layers grow forming an external shielding; the nature of the shield is similar to onion-type structures, but present much more defects derived from the folded and curved layers [14]. The disordered atomic arrangement of the amorphous phase leads to the breakage of the basal plane during the annealing at higher temperatures, resulting in the formation of the additional edges. It is important to know that the catalytic results show that the microspheres annealed at 800 °C present more ability to the isomerization reaction than the 400 °C annealed microspheres. This is probably due to the highly bended structure of the microspheres annealed at 800 °C, considering that the differences in the isomerization reactions have been related with the presence of acidic sites on the surfaces of basal planes [1, 22]. Thus, in terms of both catalyst characterizations, the lower activity and different selectivity of the ReS<sub>2</sub>-800 °C respect to its ReS<sub>2</sub>-400 °C counterpart can be explained due to the superposition of the positive effect of structural defects originated on the basal planes of bended layers, and to the negative effect of their higher stacking and longer length. A similar effect has been reported indicating the negative effect of the bending Mo(W)S<sub>2</sub> layers for the HDS performance [32].

## 4 Conclusions

In this paper we evaluate the use of a new microspherical ReS<sub>2</sub> catalyst for the hydrodesulfurization of



3-methylthiophene. The ReS<sub>2</sub> microspherical catalyst was successfully synthesized through a simple solvothermal route using elemental sulfur, Re<sub>2</sub>(CO)<sub>10</sub> and toluene as solvent. The subsequent annealing process at different temperatures plays an important role in the conformation and characteristics of the self-assembled ReS<sub>2</sub> in the microspherical hierarchical structure, and in their further catalytic properties. ReS<sub>2</sub> microspheres annealed at 400 °C are composed by an amorphous arrangement of nano-layers, while those of the sample annealed at 800 °C exhibit larger basal planes with bended and more stacked layers. The amorphous and defect-rich ReS<sub>2</sub> layers on the microsphere results in the exposure of additional edge sites, leading to an outstanding catalytic performance for the hydrodesulfurization of 3-methylthiophene. The present work indicates that the solvothermal synthesis of microspherical ReS<sub>2</sub> can be a useful pathway for the preparation of ReS<sub>2</sub> HDS catalysts.

**Acknowledgements** The authors gratefully thank CONICYT (FONDECYT GRANT 1131112), Núcleo Milenio de Magnetismo, CEDENNA, CONACYT (Projects 174689 and 117373), PAPIIT (Project IN104714-3), Supercómputo-UNAM (LANCAD-UNAM-DGTIC-041) and CONICYT Postdoctoral Project 3170761 for the different financial supports. We are also very grateful to David A. Domínguez for valuable technical help obtaining the XPS spectra.

## References

1. Sepúlveda C, García R, Reyes P, Ghampson I, Fierro J, Laurenti D, Vrinat M, Escalona N (2014) *Appl Catal A* 475:427
2. Lui H, Xu B, Lim JM, Yin J, Miao F, Duan CG, Wan XG (2016) *Phys Chem Chem Phys* 18:14223
3. Ho T, Shen Q, McConnachie J, Kliewer C (2010) *J Catal* 276:114
4. Yang L, Lu S, Wang H, Shao Q, Liao F, Shao M (2017) *Electrochim Acta* 228:268
5. Al-Dulaimi N, Lewis DJ, Zhong XL, Malik MA, O'Brien P (2016) *J Mater Chem C* 4:2312
6. Chhetri M, Gupta U, Yadgarov L, Rosentsveig R, Tenne R, Rao C (2015) *Dalton Trans* 44:16399
7. Jacobsen CJ, Törnqvist E, Topsøe H (1999) *Catal Lett* 63:179
8. Harris S, Chianelli R (1984) *J Catal* 86:400
9. Wang L, Sofer Z, Luxa J, Sedmidubský D, Ambrosi A, Pumera M (2016) *Electrochem Commun* 63:39
10. Chianelli R (1984) *Cat Rev Sci Eng* 26:361
11. Wildervanck JC, Jellinek F (1971) *J Less Common Met* 24:73
12. Tongay S, Sahin H, Ko C, Luce A, Fan W, Liu K, Zhou J, Huang YS, Ho CH, Yan J, Ogletree DF, Aloni S, Ji J, Li S, Li J, Peeters FM, Wu J (2014) *Nat Commun* 5:3252
13. Hafeez M, Gan L, Li H, Ma Y, Zhai T (2016) *Adv Funct Mater* 26:4551
14. Yella A, Therese HA, Zink N, Panthöfer M, Tremel W (2008) *ChemMater* 20:3587
15. Tu W, Denizot B (2007) *J Colloid Interface Sci* 310:167
16. Tang N, Tu W (2009) *J MagnMagn Mater* 321:3311
17. Brorson M, Hansen TW, Jacobsen CJ (2002) *J Am Chem Soc* 124: 11582
18. Aliaga JA, Araya JF, Lozano H, Benavente E, Alonso-Núñez G, González G (2015) *Mater Chem Phys* 151:372
19. Qi F, Cheng Y, Zheng B, He J, Li Q, Wang X, Yu B, Lin J, Zhang J, Li P, Zhang W (2017) *J Mater Sci* 52:3622
20. Zhang Q, Tan S, Mendes RG, Sun Z, Chen Y, Kong X, Xue Y, Rummeli MH, Wu X, Chen S (2016) *Adv Mater* 28:2616
21. Zhang Q, Wang W, Kong X, Mendes RG, Fang L, Xue Y, Xiao Y, Rummeli MH, Chen MH, Fu L (2016) *J Am Chem Soc* 138:11101
22. Mdeleni MM, Hyeon T, Suslick KS (1998) *J Am Chem Soc* 120:6189
23. Zhu G, Wang W, Wu K, Tan S, Tan L, Yang Y (2016) *Ind Eng Chem Res* 55:12173
24. Farag H, El-Hendawy ANA, Sakanishi K, Kishida M, Mochida I (2009) *Appl Catal B* 91:189
25. Farag H, Al-Megrem H (2009) *J Colloid Interface Sci* 332:425
26. Lamfers HJ, Meetsma A, Wiegers G, De Boer J (1996) *J Alloy Compd* 241:34
27. Wu Z, Wang D, Sun A (2010) *J Mater Sci* 45:182
28. Aliaga JA, Alonso-Núñez G, Zepeda T, Araya JF, Rubio PF, Bedolla-Valdez Z, Paraguay-Delgado F, Farías M, Fuentes S, González G (2016) *J Non-Cryst Solids* 447:29
29. Escalona N, Yates M, Avila P, Lopez Agudo A, Fierro J, Ojeda J, Gil Llambias F (2003) *Appl Catal A* 240:151
30. Bouyssieres L, Flores L, Pobleto J, Gil Llambias F (1986) *Appl Catal* 23:271
31. Nogueira A, Znaiguia R, Uzio D, Afanasiev P, Berhault G (2012) *Appl Catal A* 29:92
32. Guzmán MA, Huirache-Acuña R, Loricera CV, Hernandez JR, Díaz de León JN, De los Reyes JA, Pawelec B (2013) *Fuel* 103:321